Published in Journal of Contaminant Hydrology, 47, issues 2-4, 349-363, 2001
which should be used for any reference to this work

Radionuclide release and transport from nuclear underground tests performed at Mururoa and Fangataufa — predictions under uncertainty

Wilfried Pfingsten [a,*], Jörg Hadermann [a], Pierre Perrochet [b]

[a] *Paul Scherrer Institute (PSI), CH-5232 Villigen, Switzerland*
[b] *Centre d'Hydrogéologie, Neuchâtel University, CH-2007 Neuchâtel, Switzerland*

Abstract

In the context of a study by the International Geomechanical Commission (IGC) and the International Atomic Energy Agency (IAEA) on the effects of nuclear tests at the atolls of Mururoa and Fangataufa, release to the biosphere is estimated for 35 radionuclides originating from 147 nuclear underground tests. Based on a qualitatively characterised hydrogeological situation of atolls and relatively scarce site-specific data, a model chain was developed to conservatively estimate the radionuclide fluxes via groundwater, from their sources, the explosion cavities, towards the biosphere, the ocean or lagoon.

Finite element hydro-thermal modelling was used to describe water flow. Parameters were calibrated by a very few measured pre-test temperature profiles in bore holes. The impact of the tests on groundwater flow and mechanical impact on rock was considered. Estimates were made to quantify spatial extensions and temporal evolution of impact by using measurements on refilling rate of the cavities. Tests were categorised according to their specific yield and location although detailed data were missing. A base case parameter set was defined for the hydraulic conditions and for the initial radionuclide inventory of individual tests. Models were used to describe the concentration of radionuclides in the cavities as a function of time. Radionuclide transport from the cavities to the biosphere was represented by two different approaches: a double porosity model for the fractured volcanic rock and a single porosity model for the overlaying, highly porous carbonates. Results consist of conservative estimates on radionuclide release into the environment, or concentration in the lagoon or ocean water. Their sensitivity was investigated using different models and parameters. A few measured data (concentrations in a few cavities, in the deep carbonates and in the lagoons for selected radionuclides, such as ^{3}H, ^{14}C, ^{36}Cl, ^{90}Sr, ^{129}I, $^{137}Cs^{239}$, ^{240}Pu and ^{241}Am) were available for a comparison with the calculations. In view of the lack and uncertainty of site-specific data, the agreement is of acceptable quality.

Keywords: Mururoa atoll; Hydrogeologic modelling; Radionuclide transport; Nuclear tests; Data uncertainty

* Corresponding author. Tel.: +41-56-310-2418; fax: +41-56-310-2821.
E-mail address: wilfried.pfingsten@psi.ch (W. Pfingsten).

1. Introduction

After the definitive end, in 1996, of the nuclear underground tests at the atolls of Mururoa and Fangataufa, the French government asked the International Geomechanical Commission (IGC) to evaluate the mechanical stability and the hydrological situation and the International Atomic Energy Agency (IAEA) to investigate the potential radiological impact of the tests and their potential long-term effects. In order to estimate radionuclides migration rates to the biosphere, the knowledge of long-term test-induced perturbations on the hydro-thermal circulation is of prime importance. The hydrogeological system of the atolls is described in the literature (French Liaison Office, 1996; Guille et al., 1996; Henry et al., 1996), as are the mechanical effects of a nuclear explosion on the host rock (Bouchez and Lecomte, 1996; Damjanac, 1996). Schematically, the atoll consists of a volcanic basement above the ocean crust covered by carbonate formations with a relatively high permeability. The thickness of the carbonates can reach a few hundreds of metres with, at the top, a coral rim separating a 50-m deep lagoon from the ocean.

Nuclear underground tests, performed mainly in the volcanic rocks, induced a cavity and fracturing in an adjacent spherical volume. The fractured rock above the explosion location collapses and a very high permeability chimney is created (Fig. 1). The large amount of heat generated vaporises rock. Within an initial cooling phase, molten rock forms a meniscus (lava) at the bottom of the cavity while water is refilling the cavity within hours or days. The radionuclide inventory is distributed within the lava formed, sorbed on crushed rocks in the cavity or dissolved in the cavity water. Background atoll water flow pattern and disturbances induced by thermal energy and hydraulic permeability increase, in the vicinity of the test, define the radionuclide migration path.

Field data are sparse. Complete hydro-geological characterisation such as permeability, pressure and temperature profiles, as well as individual test details (yield, radionuclide inventory, depth, size of chimney or integrity or properties of the volcanic cover) are not available. Instead, mainly qualitative information on tests was offered to characterise test performances. Most of the test (121) behaved as intended, i.e., that volcanic cover on top of the chimney was intact. For some tests, Chimney Reaching Top of Volcanics (CRTV) tests, the chimney reaches the top of volcanics (12), or radionuclide leakage out of the chimneys (4) was reported, indicated by increased radionuclide concentrations measured after the test in the deep carbonates. Additional safety tests (10), some of them going critical, were performed in the carbonates and upper volcanics.

To overcome this lack of detailed data, generic hydraulic two- and three-dimensional pre-test and post-test modelling were done. Improved and/or alternate design of models

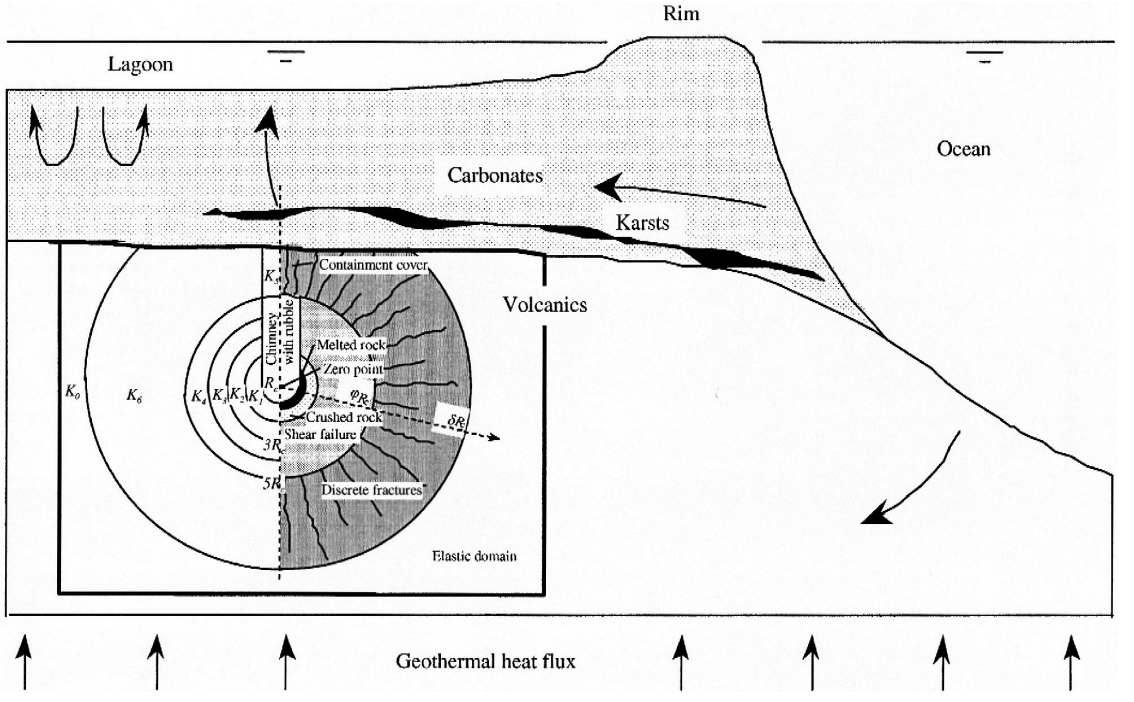

Fig. 1. Sketch of hydro-thermal circulations in a typical atoll half cross-section, rock damages generated by a nuclear explosion, where φR_c is the chimney height and δR_c maximum spreading of the permanently damaged zone, and hydraulic conductivity estimates (scenarios), K_i, made for hydro-thermal modelling. Note: the figure is not to scale. The lagoon diameter is roughly 20 km; for a 100 kt test, the depth is typically 500 m below the volcanics/carbonates interface and the extend of the damage zone $\varphi R_c \cong 280$ m.

was used and validation attempts were made, based on available field data, to evaluate model sensitivity to hydrogeological and nuclear test parameters. Yield classes were defined for the test categories. Finally, conservative scenarios were specified to derive upper bounds for the water velocities, and their sensitivity to parameters was tested. Radionuclide migration paths and distances were also deduced from qualitative information. Transport properties of radionuclides (such sorption coefficient, diffusion coefficient) were taken from the literature since site-specific data were lacking. Transport modelling includes 1D double porous and single porous medium approach to distinguish between flow in the obviously fractured volcanic rocks especially in the vicinity of the tests, and in highly porous media, like the carbonates. The first allows for relatively fast flow in the fractures and additional diffusion into the rock matrix providing a conservative estimate with respect to radionuclide travel times to the biosphere.

2. Hydraulic modelling

Natural groundwater circulation in the atoll is essentially governed by buoyancy forces due to the geothermal flux heating the system from below (Fig. 1). Cold and dense ocean water penetrates from the outer slopes of the atoll inward, is heated and rises through the volcanics and carbonates toward the lagoon. This atoll typical flow regime is called 'endo-upwelling'. The phenomenon is particularly marked in the carbonate formations where the high permeabilities allow important, almost horizontal centripetal fluxes of water with vertical flow in the centre. In the absence of any hydraulic testing at the atolls, and considering a few measurements of hydraulic conductivity on core samples giving values smaller or equal to 10^{-10} m/s, the only parameter that could be used to calibrate the pre-test hydraulic model was the temperature. Vertical temperature profiles for two non-specified locations, below the rim and the lagoon, respectively, indicate a laterally, tidal-influenced flow in highly transmissive karst layers within the carbonates allowing for direct water exchange to the ocean. These temperature profiles were calibrated at atoll scale by 2D- and 3D-coupled hydro-thermal modelling (Perrochet and Tacher, 1998) using the software FEFLOW, (Diersch, 1996a,b). Parameter variation and analysis lead to parameter values consistent with observation and former modelling studies with one exception: for the flow field below the rim in the upper carbonates local flow systems evolved which was explained by the much finer grid in our calculations. The general findings for the pre-test hydraulic conditions are average permeabilities in the volcanic rocks of about 10^{-7} and 10^{-4}–10^{-5} m/s in the carbonates. Sensitivity studies on parameters for hydraulic conductivity variations, location of lower boundary or geothermal heat flux allow several acceptable parameter sets (Table 1); resulting Darcy fluxes are in the range of mm/year in the volcanics to m/year in the carbonates. In the karst layer, horizontal Darcy fluxes can be as high as 15–20 m/year.

Numerical modelling was also used to assess the impact of nuclear tests (Perrochet and Tacher, 1998). Their influence is local and does not change the global flow pattern in the atoll. Locations and depth of individual nuclear tests were not available. This

Table 1
Numerical values of given or assumed hydro-thermal parameters for pre-test situation

	Carbonates	Volcanic
Matrix parameters		
Hydraulic conductivity K_o [m/s] (given)	10^{-5}–10^{-4} (10^{-3})	10^{-7} (10^{-6}–10^{-8})
Porosity [−] (given)	0.3–0.4	0.1
Compressibility S_o [m^{-1}] (assumed)	10^{-5}–10^{-4}	10^{-5}–10^{-4}
Thermal conductivity λ_s [J m^{-1} s^{-1} K^{-1}] (given)	2.0	2.5
Volumetric heat capacity $(\rho c)_s$ [10^6 J m^{-3} K^{-1}] (given)	2.2	2.2
Thermal longitudinal dispersivity α_L [m] (assumed)	10	10
Thermal transverse dispersivity α_T [m] (assumed)	1	1
Solute longitudinal dispersivity α_L [m] (assumed)	10–100	10–100
Fluid and other parameters		
Salinity C_o (assumed constant)	34 g/l	
Thermal conductivity λ_l	0.65 J m^{-1} s^{-1} K^{-1}	
Volumetric heat capacity $(\rho c)_l$	$4.2 \cdot 10^6$ J m^{-3} K^{-1}	
Reference temperature T_o (given ocean surface temperature)	26°C	
Geothermal heat flux	4500 (3000) J d^{-1} m^{-2}	
Lower boundary at	−1200 (−2000) m	

information is indeed fundamental since it directly determines the thickness of the volcanic containment cover and, thus, the flow rates toward the carbonate formations. In the absence of more precise information, and given the uncertainty on the actual height of collapse chimneys, near-field sensitivity and conservative analyses were carried out in terms of containment cover thicknesses and sensitivity of its conductivity. In the models, explosions are implemented either at the centre of the atoll (2D axi-symmetric simulations) or below the rim (3D simulations).

According to literature and results of the IGC Stability Subgroup (Damjanac, 1996; Fairhurst et al., 1998), the schematisation of collapse chimneys and adjacent damaged zones is done as indicated in Fig. 1 and parameters are given in Table 2. The cavity radius is given by $R_c = 12\ Y^{1/3}$ where Y is the yield in kt. Thermal energy deposition was estimated to yield the increase of the groundwater temperature. A reasonable average temperature increase in the range 25–50°C was assumed, yielding possible initial (after resaturation) chimney temperatures in the range 55–80°C for transient hydrodynamic simulations. The thermal drive dissipates after some hundreds of years. Therefore, groundwater flow and related radionuclide transport modelling can be divided into a short-term transient period up to a few hundreds of years taking into account increased vertical upward water velocities, and a steady-state groundwater flow regime, as before the tests, including the increased permeability areas at the test locations. As several near-field permeability variations were acceptable, when compared with data from refilling of the chimneys (Fig. 2), a testspecific transient Darcy flux was hard to quantify. Fig. 2 (left, 14.5 kt test), indicates that variation F0 and F2 compare well with measured filling rates. The curve deduced from the observations from a 3.2 kt test

Table 2
Post-test hydraulic conductivity distributions [m/s] in the damaged zones and related Darcy flux

	F0[a]	F1[a]	F2[a]	F3[a]	Radii, distance to centre of explosion
K_0	10^{-7}	10^{-7}	10^{-7}	10^{-7}	volcanics, distance $> 10R_c$
K_1	10^{-7}	10^{-5}	10^{-7}	10^{-3}	$R_c - 2R_c$
K_2	10^{-7}	$5 \cdot 10^{-6}$	10^{-7}	$5 \cdot 10^{-4}$	$2R_c - 3R_c$
K_3	10^{-7}	10^{-6}	10^{-7}	$5 \cdot 10^{-4}$	$3R_c - 4R_c$
K_4	10^{-7}	$5 \cdot 10^{-7}$	10^{-7}	$5 \cdot 10^{-4}$	$4R_c - 5R_c$
K_5	10^{-7}	10^{-6}	10^{-6}	10^{-4}	volcanic cover
K_6	10^{-7}	10^{-7}	10^{-7}	10^{-4}	$5R_c - 10R_c$

Simulation set-up	Related peak Darcy flux [m/year] in/on top of the cover[b]			
5 kt test, $\Delta T = 25$°C, 15-m cover	0.012 (0.03)	1.2 (0.3)	0.5 (0.15)	
5 kt test, $\Delta T = 50$°C, 15-m cover	0.2	3.2	1.2	
150 kt test, $\Delta T = 25$°C, 100-m cover	0.09	1.2	0.6	
150 kt test, $\Delta T = 50$°C, 100-m cover				20–70
150 kt test, $\Delta T = 50$°C, no cover	45			58
150 kt test, $\Delta T = 50$°C, no cover, 3D	35			
150 kt test, $\Delta T = 50$°C, no cover, 3D and 10-m karst layer	2–5			

F0–F3 denote variations.

[a]Assumed hydraulic conductivities [m/s] for: carbonates 10^{-4}, 10-m thick karst layer 10^{-2}, chimney 10^{-2}, rock lava 10^{-9}.

[b]Quasi steady state (> 500 year after the tests) Darcy fluxes are given in parenthesis; note that the average pre-test flux is 0.008 m/year.

(Fig. 2, right) exhibits slope changes that cannot be captured by any of the tested permeability variations. However, a fairly good match is obtained this time with variation F1.

Near-field thermo-hydraulic modelling show for all parameter variations that local flow systems develop in and around the chimney. The near-field simulations have shown thermal convection of water always dominating in the collapse chimneys, highly unstable (unsteady or periodic) during a few years after the test; and, at the end of the cooling period, the persistence of convection cells within the collapsed chimney. Hence, chimneys may be considered as well mixed reactors at all times. In order to provide both probable and worst-case results for source term and transport calculations, special focus was on the assumption of hydraulic conductivity of the volcanic cover. Sensitivity was performed to estimate conservatively maximal possible Darcy fluxes for different types of tests performed. To estimate the total impact of the test, successive simulations with hydraulic conductivities of 10^{-6}, 10^{-5} and 10^{-4} m/s in the damaged zones were investigated. The temperature in the carbonates above the chimney is increased by a maximum of 1–2°C in the vicinity of the interface to the volcanics. This does not alter the regional flow field and the vertical fluxes in the carbonates are of the order of 2–3 m/year at all times. Pre-test, steady-state total discharge into the lagoon is of the order of 60 000 m^3/day. This value is basically insensitive to the presence of all tests. With

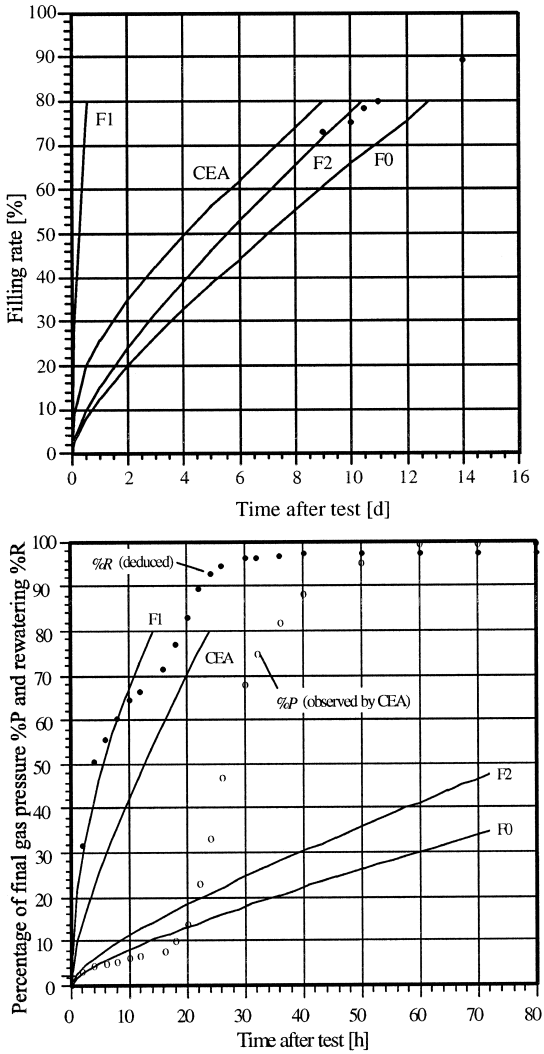

Fig. 2. Comparison of measured filling rates (dots) for a 14.5 kt-test (top) and for a 3.2 kt-test (filling rates, $\%R$, black dots, deduced from pressure measurements, $\%P$) to rates simulated with four permeability scenarios (solid lines). F1 has higher permeabilities than F2 for distances in between R_c and $4R_c$.

hydraulic conductivities of 10^{-4} m/s in all the damaged zones, the total discharge into the lagoon is increased by less than 1%.

3. Source term

The radionuclide concentration in the water leaving the vicinity of the test depends on the test type (fuel, device set-up), its geochemical behaviour and the volume in which

Table 3
Parameters for calculations of different test yields and test characteristics

Nuclide	Generic test yield of 150 kt and			10 kt	Cluster of different test yield [kt] and related inventory [TBq]									
	K_D [m^3/kg]	matrix depth [m]	v_D [m/year][a] (volcanic)	v_D [m/year][a] (volcanic)	normal and CRTV, 5	normal 25	normal 60	normal 100	Enee 53	Lycos 87	Megaree 54	Nestor 47	v_D [m/year][b] (volcanic)	
^{3}H	0	(0.0495) 0.01	1 (0.1,10)	1	1300	2668	5256	8200	4770	7134	4860	4230	20 (2)	20 (2)
^{14}C	0	0.0495	1	1	0.2			0.25		0.25			20 (2)	20 (2)
^{36}Cl	0	(0.0495) 0.01	1	1	0.0016			0.045		0.039			20 (2)	20 (2)
^{55}Fe	0.01/0.03	(0.0495)0.01	1	1	76			1500		1305			2	2
^{59}Ni	0.01/0.03	0.0495			0.006			0.12		0.1			2	2
^{60}Co	0.01/0.03	(0.0495) 0.01	1	1	200			4100		3567			2	2
^{63}Ni	0.01/0.03	(0.0495) 0.01	1	1	0.75			15		13.05			2	2
^{79}Se	0/0.01	(0.0495) 0.01	1	1	$1.5\cdot10^{-5}$			$3.9\cdot10^{-4}$		$3.4\cdot10^{-4}$			20 (2)	20 (2)
^{90}Sr	0.008/0.1	(0.0495) 0.01	1 (0.1,10)	1	11	114.1	302	520	265	452	270	235	20 (2)	20 (2)
^{93}Zr	0.05	0.0495			$4\cdot10^{-4}$			0.011		0.0096			2	2
^{99}Tc	0/0.01	(0.0495) 0.01	1	1	0.0045			0.083		0.072			20 (2)	20 (2)
^{106}Ru	0.01/0.03	(0.0495) 0.01	1	1	680			2700		2349			2	2
^{107}Pd	0.05	0.0495			0.001			0.0035		0.003			2	2
^{121}Sn	0.01/0.03	0.0495			0.0029			0.0038		0.0033			2	2
^{125}Sb	0/0.01	(0.0495) 0.01	1	1	10			120		104.4			20 (2)	20 (2)
^{126}Sn	0.01/0.03	(0.0495) 0.01	1	1	$4.2\cdot10^{-4}$			0.0043		0.0037			2	2
^{129}I	0	(0.0495) 0.01	1	1	$1.5\cdot10^{-5}$			$1.7\cdot10^{-4}$		$1.7\cdot10^{-4}$			20 (2)	20 (2)
^{134}Cs	0.3	(0.0495) 0.01	1	1	0.077			0.1		0.1			2	2
^{135}Cs	0.3	(0.0495) 0.01	1	1	$5.2\cdot10^{-4}$			0.0085		0.0074			2	2
^{137}Cs	0.3	(0.0495) 0.01	1 (0.1,10)	1	35	156.1	365.7	600	318	522	324	282	20 (2)	20 (2)
^{147}Pm	0.05	(0.0495) 0.01	1	1	110			2400		2088			2	2
^{151}Sm	0.05	(0.0495) 0.01	1	1	1.4			15		13.05			2	2
^{152}Eu	0.05	(0.0495) 0.01	1	1	2.8			56		48.7			2	2
^{154}Eu	0.05	(0.0495) 0.01	1	1	0.55			11		9.6			2	2
^{155}Eu	0.05	(0.0495) 0.01	1	1	7			36		31			2	2

^{236}U	0.01	(0.0495)	0.01	1	1	$7.2 \cdot 10^{-4}$			0.0026		0.0023			2	2
^{237}Np	0.2/0.5	(0.0495)	0.01	1	1	$5.6 \cdot 10^{-4}$			0.0042		0.0037			2	2
^{238}Pu	0.5	(0.0495)	0.01	1	1	1.6			1.6		1.6			2	2
^{239}Pu[c]	0.5	(0.0495)	0.01	1	1	7.9	7.9	7.9	7.9	7.9	7.9	7.9	7.9	2	2
^{240}Pu	0.5	(0.0495)	0.01	1	1	2.1			2.1		2.1			2	2
^{241}Pu	0.5	(0.0495)	0.01	1	1	85			85		85			2	2
^{241}Am	0.05	(0.0495)	0.01	1	1	2.7			2.7		2.7			2	2
^{242}Pu	0.05	(0.0495)	0.01	1	1	$6 \cdot 10^{-5}$			$6 \cdot 10^{-5}$		$6 \cdot 10^{-5}$			2	2
chain 241	nuclide specific	(0.0495)	0.01	1	1									2	2

Values in parentheses are variations to the base case.

[a] For generic and normal tests.

[b] For CRTV and leaky tests (Enee, Lycos, Megaree, Nestor).

[c] Additional calculations were done for specific test categories for ^{239}Pu: safety trials in the carbonates (Cat. 4) including variation of Darcy flux and model approach: double or single porous medium; safety trials in the carbonates without nuclear yield (Cat. 5) for varying Darcy flux, device–groundwater interaction cross-section (20 m^2 and 45 m^2) and Pu solubility limit (10^{-7} and 10^{-9} mol/l); safety trials in the volcanics without nuclear yield (Cat. 6) with same sensitivity analysis as for (Cat. 5); release from 1200 m deep waste shaft (Cat. 7).

the radionuclides will be dispersed shortly after the test. There are four compartments from which radionuclides may be released: rock lava, chimney water, chimney rubble or a nuclear test device that did not go critical. Molten rock lava, forming a low permeable meniscus at the bottom of the cavity, contains refractory fission and activation products to various ratios of total nuclide inventory. The determination of the initial radionuclide partition was done in the IAEA study (IAEA, 1998). The temporal development of the radionuclide concentration in the chimney water needed some further model and parameter assumptions. The lava will dissolve during some 10 000 to several hundreds of thousands of years, and congruent release into the chimney is assumed. It contributes to a radionuclide concentration within the chimney water determined by the elemental solid/liquid distribution coefficient. Only few data on distribution coefficients were available, so we use ranges of values based on literature. We developed analytical solutions to describe the source term for the transport calculations taking into account radionuclide properties, chimney geometry and upward flow conditions from the chimney into the carbonates. For sorbing radionuclide chains distributed between lava, rubble and water, we refer to the literature (Hadermann and Pfingsten, 1998). As an example, we give here the concentration for non-sorbing nuclides (e.g., tritium)

$$C = C_0 \mathrm{e}^{\frac{\lambda b H_c \varepsilon t + v_{bg} b t + v_{bomb}(1 - \mathrm{e} - bt)}{b H_c \varepsilon}}, \qquad (1)$$

where ε is the porosity in the cavity, λ the nuclide's decay constants, v_{bomb} is the velocity increase due to the explosion's thermal impact, b a constant describing the relaxation to pre-test flow conditions, v_{bg} the background flow velocity and C_0 the initial concentration in the chimney water at $t = 0$, i.e., when resaturation was reached.

Source terms were calculated for 35 nuclides including a nuclide chain, for several Darcy flow conditions and test categories (see Table 3). The 121 "normal" tests were clustered in yield classes of 5, 25, 60 and 100 kt (and generic tests of 10 and 150 kt) performed at depth of 25, 75, 100, 150 and 250 m. For tests with a leaky cover, or

Table 4
Comparison of CEA and IAEA measurements in chimney water with results of present calculations (all concentrations are in Bq/m^3)

Nuclide	Measured					Calculated initial concentration
	LYCOS[a]	CETO[b]	ARISTEE[a,b]	BOROS[a]	AJAX[a]	
^{3}H	$5.5 \cdot 10^{9}$	$2 \cdot 10^{10}$	10^{10}	$4 \cdot 10^{8}$		10^{10}
^{90}Sr	$4 \cdot 10^{5}$	$3 \cdot 10^{5}$	$8 \cdot 10^{5}$	10^{7}	$7 \cdot 10^{5}$	$6 \cdot 10^{5}/8 \cdot 10^{6}$
^{137}Cs	$1.4 \cdot 10^{5}$	10^{4}	$2 \cdot 10^{5}$	$2 \cdot 10^{6}$	$1.3 \cdot 10^{6}$	$2.5 \cdot 10^{5}$
^{129}I		17	45			100
^{239,240}Pu		0.3	0.2			$4 \cdot 10^{3}$
^{36}Cl		$3 \cdot 10^{4}$	$3 \cdot 10^{3}$			$1 \cdot 10^{4}$
^{14}C		10^{3}	< 50			$3 \cdot 10^{6}$
^{241}Am		0.2	0.1			$1 \cdot 10^{4}$

[a] French Liaison Office (1996).
[b] IAEA (1998).

where the chimney reached the carbonates, a direct release from the chimney into the carbonates was assumed. For safety tests with (of about 0.2 kt) and without nuclear yield, different source terms were applied. Those with nuclear yield were handled like normal test but with higher Darcy flux in the carbonates. For safety test without nuclear yield device material, plutonium, was considered to dissolve at solubility limit in a cross-section where groundwater flows. Solubility limit, cross-section and water velocity were varied. The same assumption was applied to plutonium leaching from 1200-m deep waste shafts. A comparison of calculated and measured radionuclide concentration in the chimney (Table 4) yielded acceptable agreement, except for Pu and Am. Two main reasons for overestimation of Pu and Am concentration can be hypothesised. Firstly, much more than the conservatively assumed amount of 95% of these nuclides is captured in the lava (some measurements indicate that 99.9% of Pu and other actinides are trapped in the lava, IAEA, 1998). Secondly, the assumed sorption values (Table 3) are much too low for Pu and Am. These specific parameter uncertainties for Pu and Am, and also for other sorbing actinides, may easily result in an overestimation of two to three orders of magnitude for the predicted concentration in the chimney. Keeping in mind that calculated values were deduced from synthetic data and generic values for the atolls: estimates based on empirical equations for chimney geometry, nuclide inventory and distribution on possible source compartments and probable hydro-thermal scenarios, this was a gratifying result.

4. Transport

Transport in the volcanics was described by a double porosity medium approach in view of the fractures induced by the tests and the natural fractured volcanic rocks. This approach is also conservative with respect to water flow velocities and related travel times for nuclides entering the carbonates. The model includes 1D advective–dispersive transport in fractures, perpendicular matrix diffusion, sorption, decay and build-up (Jakob, 1997). Due to higher porosity in the carbonates (0.3 compared to 0.1 in the volcanics) and their genesis, we chose a single porosity model for the carbonates. A comparison was made for a double porosity approach for plutonium migration from a critical safety test in the carbonates. The double porosity approach delivers earlier breakthrough, but maximum level and time were comparable indicating that the matrix will quickly be saturated, and transport became similar to that in a single porous medium (Hadermann and Pfingsten, 1998). To quantify the total nuclide release to the carbonates and the lagoon, several approximations have to be made. Because depths of individual tests were not known, travel times were calculated by defining representative test clusters. Then, all tests were assumed to be performed at the same time, in order to get a maximum total release into the carbonates and the lagoon, i.e., to maximise the consequences. This approximation is conservative and causes higher and sharper peak releases as particularly shown for ^{3}H for a series of tests (Pfingsten and Hadermann, 1999).

Results of calculations for the most dominant tests, for which the approximate test area was given, are shown in Fig. 3 for ^{3}H, ^{90}Sr and ^{137}Cs. The calculated releases into

carbonates were transformed to concentrations in the deep carbonates to allow for a comparison with measurements, available for a few observation wells in the carbonates at Mururoa. Using the total water flow into the lagoon of 60 000 m^3/day, as calculated

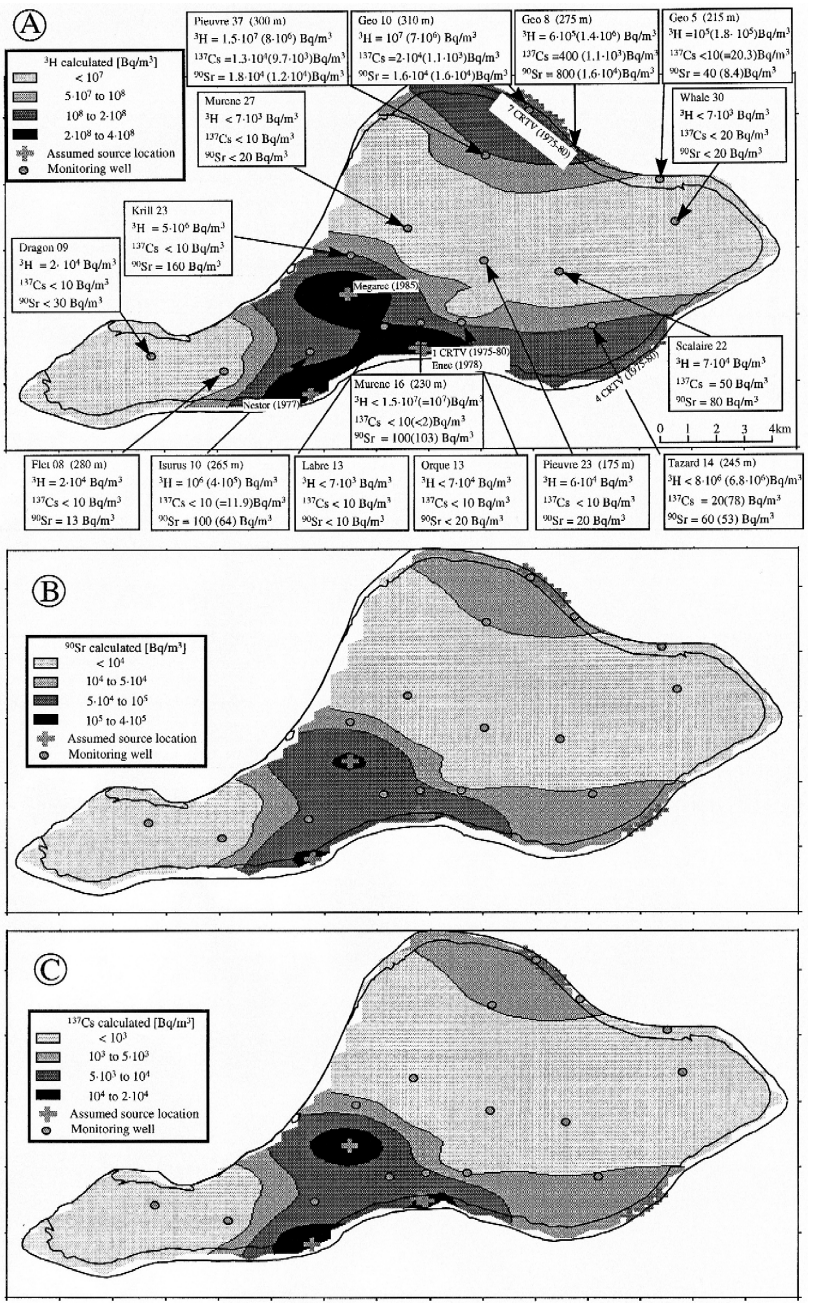

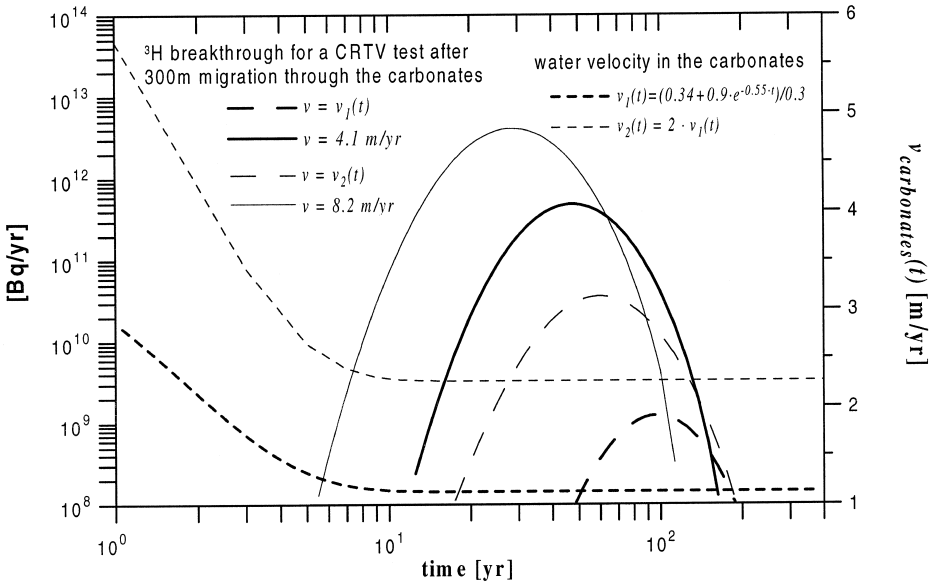

Fig. 4. Tritium breakthrough curves on top of the carbonates (left scale) for differently dissipating vertical water flow velocities (right scale) and for constant maximum velocity. The data are for a 5 kt CRTV test.

from hydro-thermal modelling, and assuming further that most of this water enters the atoll in the deeper, highly conductive carbonates and by horizontal inflow within the karst layers in the deeper carbonates, and from the volcanics, we convert calculated radionuclide releases [Bq/year] for the dominant leaky and CRTV tests into concentrations. Here, a good mixing of water in the deep carbonates is assumed. The calculated concentrations overestimate the measured concentrations, especially for those calculations with a high upward Darcy flux (20 m/year), i.e., the leaky test with a non-intact volcanic cover. Furthermore, the unknown influence of tides in the carbonates was ignored except for the assumption of mixing. This approximation neglects retardation of sorbing nuclides and overestimates concentrations. With respect to the measured concentrations, one should keep in mind that sampling in the wells was performed in depths varying from 175 to 310 m at Mururoa. As shown in Fig. 3, the peak maximum for CRTV tests are in the range of the measured concentrations. The lateral extension of the nuclide plumes in the deep carbonates may give some indication for main trends but

Fig. 3. Calculated maximal ^{3}H (A), ^{90}Sr (B) and ^{137}Cs (C) concentrations in the deeper carbonates at Mururoa in comparison to measurements in observation wells at different depth (French Liaison Office, 1996), in parentheses measurements performed by IAEA in 1997 (IAEA, 1998); $^{239,240}Pu$ was always below detection limit (0.05 Bq/m^3). Calculations were done for dominant test only and are based on conservative estimates concerning upward Darcy fluxes of 20 m/year for CRTV and leaky tests Enee, Megaree and Nestor (Hadermann and Pfingsten, 1998) and the assumption of good water mixing in the deep carbonates due to high horizontal water flow velocities and tidal effects. Levels are generally three to four orders of magnitude lower than those measured in the chimneys.

without knowledge of exact spatial coordinates of the tests and related migration paths, these are only trends. Concentrations above locations for leaky tests are overestimated which may have several explanations. Assumed upward Darcy fluxes are too high (decreasing Darcy fluxes in source term calculations by an order of magnitude will also decrease nuclide fluxes and concentrations, respectively, see sensitivity analysis in Hadermann and Pfingsten, 1998), the migration times from the cavity to the individual observation level were larger than assumed (this would especially influence predictions for sorbing nuclides) or tidal effects were underestimated (dilution would be higher).

For most of the transport calculations, constant maximum upward velocities (slightly higher than pre-test values) were chosen as conservative approximations. To estimate the conservativity, we compared the results for such an approach with those where the time dependency was explicitly taken into account as well in the source term (Eq. (1)), as in the transport. The example, presented in Fig. 4, is for a 5 kt CRTV test and short-lived ^{3}H: dissipating flow velocity gave more than an order of magnitude lower concentration levels than the constant velocity case. For sorbing radionuclides, the initial transient phase can be neglected due to its short duration and corresponding small migration distances.

5. Conclusions

The evaluation of the consequences of nuclear testing on the atolls in the South Pacific offered the possibility to apply and test many of the models developed for civilian waste management on a scale which is not accessible in usual field experiments. Comparison of pre-test thermal-hydraulic modelling, transient near-field conservative case estimations and steady-state simulations, including the impact of all the collapse chimneys and their adjacent damaged zones with increased hydraulic conductivity, allowed for estimating the long-term flow field. Estimations of radionuclide source term were mainly based on synthetic and generic data. Approximations had to be made to overcome complex transient near-field patterns. Comparison to a few measured nuclide concentrations in chimneys gave gratifying good agreement except for C, Pu and Am. For these, we have apparently underestimated sorption and the quantity of the total inventory in the lava. The combined conservativity yielded a strong overestimate of concentrations in the chimney in accordance with the overall aim of the IAEA study. Transport calculations showed that the dominant releases came from a few tests that did not perform as assumed. Calculations of releases to the carbonates from these tests were consistent with the measurements from a few bore holes. In case of ^{3}H, the impact of assuming a constant maximum Darcy flux during the transient cooling period for a specific test could be estimated, giving a rough idea of the uncertainty of calculations for other nuclides or test types. The calculated radionuclide releases to the biosphere were dominated by a few tests as indicated by a few available measurements in the carbonates and the lagoon waters. Overall, the modelling showed that peak release of non-sorbing nuclides has already occurred in the past; sorbing long-lived nuclides will reach the biosphere far in the future at low levels, whereas sorbing short-lived nuclides will decay in the underground. Though little site-specific data were available, standard model

concepts on nuclide transport could be applied and yielded acceptable agreement when compared to few existing measurements. Migration in the carbonates could not be described in a near-realistic manner due to the lack of concepts for tide-driven transport in karst systems. This problem, as others, were avoided by using (probably too) conservative assumptions.

Acknowledgements

We would like to thank members of the IGC and IAEA working groups, especially L.E. de Geer, G. de Marsily, C. Fairhurst, D.M. Levins, H. Nitsche and L. Townley as well as J.F. Sornein and his colleagues at CEA for scientific discussions throughout the project.

References

Bouchez, J., Lecomte, R., 1996. The Atolls of Mururoa and Fangataufa (French Polynesia): II. Nuclear Testing —Mechanical, Lumino-thermal and Electromagnetic Effects. CEA /DAM, Paris, France.

Damjanac, B., 1996. Numerical Simulation of the Near-field Response of a Rock Mass to an Underground Nuclear Explosion. Itasca Consulting Group.

Diersch, H.J., 1996a. FEFLOW —Physical Basis of Modeling. WASY, Berlin.

Diersch, H.J., 1996b. Interactive, Graphics-based Finite Element Simulation System FEFLOW for Modeling Groundwater Flow, Contaminant Mass and Heat Transport Processes. WASY, Berlin.

Fairhurst, C., Brown, E.T. et al., 1998. Stability and Hydrology Issues Related to Underground Nuclear Testing at French Polynesia. IGC, Paris.

French Liaison Office, 1996. Study of the radiological situation at the atolls of Mururoa and Fangataufa (Doc. 1 to 11). Ministre des Defences, Direction des Centre D'experimentations Nucleaires, Commissariat a l'Energie Atomique, CEA/DAM, Paris.

Guille, G., Goutiere, G. et al., 1996. The Atolls of Mururoa and Fangataufa (French Polynesia): I. Geology–Petrology–Hydrogeology, from Vulcano to Atoll. CEA/DAM, Paris, France.

Hadermann, J., Pfingsten, W., 1998. Source term and geosphere transport calculations for the atolls of Mururoa and Fangataufa. Technical Report TM-44-98-06, Paul Scherrer Institute, Villigen, Switzerland. Also available for download at: http://www1.psi.ch/~curti/Frameset_home.html.

Henry, P., Guy, C. et al., 1996. A convective model of water flow in Mururoa basalts. Geochimica et Cosmochimica Acta 60, 2087–2109.

IAEA, 1998. The Radiological Situation at the Atolls of Mururoa and Fangataufa —Summary Report and Technical Report 1–7. Vienna, IAEA.

Jakob, A., 1997. Modelling solute transport using the double porous medium approach, Modelling in Aquatic Chemistry. OECD Nuclear Energy Agency, Paris.

Perrochet, P., Tacher, L., 1998. Mathematical modelling of hydrothermal processes at Mururoa atoll, Documentation Francaise. Ecole Polytechnique Federale de Lausanne, Lausanne, Switzerland.

Pfingsten, W., Hadermann, J., 1999. PSI contribution to the IAEA study on the radiological situation at the atolls of Mururoa and Fangataufa. Scientific Report 1998, vol. IV (79–91), Paul Scherrer Institute, Villigen, Switzerland.